J Appl Electrochem (2008) 38:613–617
DOI 10.1007/s10800-008-9479-5

ORIGINAL PAPER

Comparative study of the preparation and electrochemical performance of $LiNi_{1/2}Mn_{1/2}O_2$ electrode material for rechargeable lithium batteries

F. Lian · P. Axmann · C. Stinner · Q. G. Liu · M. Wohlfahrt-Mehrens

Received: 29 November 2006 / Revised: 17 December 2007 / Accepted: 7 January 2008 / Published online: 19 January 2008

Abstract Positive electrode material $LiNi_{1/2}Mn_{1/2}O_2$ was synthesized via the carbonate co-precipitation method and the hydroxide precipitation route to study the effects of the precursor on its structural and electrochemical properties. The results of X-ray diffraction and Rietveld refinement show that the carbonate precursor of Ni^{2+} and Mn^{2+} exhibits one phase at a pH of 8.5, while the hydroxide deposit separates into $Ni(OH)_2$ and $Mn(OH)_2$ phases under the same experimental conditions. $LiNi_{1/2}Mn_{1/2}O_2$ material prepared from the hydroxide precursor shows 8.9% Li/Ni exchange and a large capacity loss of 11.3% in the first 10 cycles. By contrast, more uniform distribution of transition metal ions and stable Mn^{2+} in the carbonate precursor contribute to only 7.8% Li/Ni disorder in the obtained $LiNi_{1/2}Mn_{1/2}O_2$, which delivers a reversible capacity of about 182 mAh g^{-1} at a current rate of 14 mA g^{-1} between 2.5 and 4.8 V.

Keywords Carbonate co-precipitation method · Li/Ni disorder · Reversible capacity · Rietveld refinement · Uniform distribution of Ni^{2+} and Mn^{2+}

1 Introduction

Recently, $LiNi_{1/2}Mn_{1/2}O_2$ has emerged as a promising cathode material for advanced rechargeable lithium batteries [1]. The material offers high theoretical capacity ($\sim$280 mAh g^{-1}), and significantly enhanced structural stability, because Mn ions maintain an oxidation state of +4 during electrochemical cycles [2–3].

Study of $LiNi_{1/2}Mn_{1/2}O_2$ can be traced back to an approach to the electronic stabilization of $LiMnO_2$ using $LiNi_{1-y}Mn_yO_2$ ($0 < y \leq 1/2$) [4]. After 1992 the electrochemical performance of $LiNi_{1/2}Mn_{1/2}O_2$ material was optimized further. The transition metal double hydroxide (i.e. $(Ni,Mn)(OH)_2$) route is believed to have accessibility for a homogeneous distribution of transition metal ions and is widely used [5–7]. As-obtained $LiNi_{1/2}Mn_{1/2}O_2$ reported by Spahr et al. [8], delivered a capacity of 150 mAh g^{-1} falling to 125 mAh g^{-1} after 25 cycles at 0.38 mAc m^{-2}, while Ohzuku [9] proposed a material with 170 mAh g^{-1} at 0.17 mA cm^{-2} for 30 cycles. The facts suggest that the specific capacity and other electrochemical properties of $LiNi_{1/2}Mn_{1/2}O_2$ depend critically on the synthesis process and charge/discharge rate [10]. Moreover, it is found that manufactured $LiNi_{1/2}Mn_{1/2}O_2$ samples exhibit differing values for Li/Ni exchange (commonly 8–12%) depending on their synthesis route [7–11]. Recent research into $LiNi_{1/2}Mn_{1/2}O_2$ shows that Li/Ni disorder greatly limits the opening of Li slab space [2] leading to exponential decrease in Li diffusivity and thus the deterioration of electrochemical properties. These observations clearly indicate that the electrochemical performance of $LiNi_{1/2}Mn_{1/2}O_2$ can be improved by optimizing its synthesis method to reduce the Li/ Ni disorder.

Additionally, manganese with oxidation states beyond the bivalence in the precursor may introduce impurities such as Mn_2O_3 and MnO_2 into the final product, resulting in poor electrochemical reactivity [12]. Therefore, the purity of the precursor plays a significant role in the quality of the targeted material. From this point of view, carbonate co-precipitation can be used to prepare pure $LiNi_{1/2}$

F. Lian (✉) · Q. G. Liu
Department of Materials Science and Engineering, University of Science and Technology Beijing, Beijing 100083, China
e-mail: lianfang@mater.ustb.edu.cn

F. Lian · P. Axmann · C. Stinner · M. Wohlfahrt-Mehrens
Centre of Solar Energy and Hydrogen Research (ZSW) Baden-Württemberg, Helmholtzstr. 8, Ulm 89081, Germany

$Mn_{1/2}O_2$ material due to the stability of the $MnCO_3$ precursor [13].

We synthesize the precursor via the carbonate co-precipitation route and the hydroxide precipitation method for comparison. The dense $LiNi_{1/2}Mn_{1/2}O_2$ sample is prepared by a two-step calcination technique [14, 15]: the precalcine of the precursor and final sinter of the resulting oxide mixed with stoichiometric $LiOH{\cdot}H_2O$. The precursor and final material are investigated using scanning electron microscopy (SEM), powder X-ray diffraction methods (XRD) and Rietveld refinements.

2 Experimental

$LiOH{\cdot}H_2O$ (98%+, Aldrich), Li_2CO_3 (99%+, Fluka), $Ni(NO_3)_2{\cdot}6H_2O$ (98%+, Fluka), and $Mn(NO_3)_2{\cdot}6H_2O$ (97%+, Fluka) were used as the starting material. Lithium carbonate or hydroxide and a mixed aqueous solution of manganese nitrate and nickel nitrate were simultaneously added dropwise into a reactor, in which distilled water was under vigorous stirring. In both cases, the pH value in the reactors was controlled at 8.5. The obtained slurry was carefully filtered and washed three times using a centrifuge. The precursor was dried in a vacuum oven overnight at 120 °C and preliminarily annealed at 450 °C for 10 h in air. The precalcined precursor was mixed with stoichiometric $LiOH{\cdot}H_2O$ using a mortar and pestle, and finally sintered at 900 °C for 12 h in air. The heating and cooling rates were fixed at 3 °C min^{-1}.

The precise cation composition of samples was determined by inductively coupled plasma optical emission spectroscopy (Spectroflame ICP, 2.5 KW, 27 MHz). The results in weight percent were converted to atomic percent and then ultimately converted to stoichiometry, where the total content of Ni and Mn was normalized to 1 and the oxygen content was assumed at 2.

The samples were characterized by XRD using a Siemens D5000 diffractometer with Cu Kα radiation at 40 kV, 300 mA, with the step of 0.02° and scanning time of 1 s per step. Detailed structure testing was carried out with a scanning step of 0.01° and scanning time of 18 s per step. The structure refinement was performed with the Topas calculation program. The morphology of the precursor and $LiNi_{1/2}Mn_{1/2}O_2$ material were observed by SEM (LEO VP 1530).

The electrochemical properties of $LiNi_{1/2}Mn_{1/2}O_2$ were studied in half-cells. The positive electrode was prepared by pressing a mixture of 60% active material, 20% acetylene black and 20% PTFE into aluminum mesh as the current collector and dried under vacuum at 150 °C overnight. The electrodes were assembled in an argon-filled glove box with lithium foil as counter and reference electrode, and 1 M $LiPF_6$ solution in EC/DEC (1:1 in volume) as electrolyte. Cells were cycled at room temperature in galvanostatic mode at a constant C/20 rate, corresponding to a theoretical exchange of one electron per preparation during charge and discharge.

3 Results and discussion

3.1 Precursor

The X-ray diffraction patterns and morphology of the precursors produced are given in Fig. 1. In Fig. 1a the vertical upper ticks represent the position of the $NiCO_3$ (JCPDS No.12-0771) phase reflection, while the lower ticks correspond to the reflex position of $MnCO_3$ (JCPDS No.44-1472). The co-precipitated carbonate is a single phase and no remarkable secondary phase can be observed in the patterns, which indicates the complete intersolubility of $MnCO_3$ and $NiCO_3$. Moreover, the patterns can be indexed base on the hexagonal structure of $MnCO_3$ (space group R-3c), where the broad integrated diffraction peaks are attributed to intercalation of Ni^{2+} into the host structure. In addition, the relatively stable divalent manganese ions in aqueous carbonate solution make the process easy to control. Using ICP analysis, the average chemical composition is determined to be $[Ni_{0.501}Mn_{0.499}]CO_3$, which agrees with the desired composition within experimental uncertainty.

The Ni and Mn ions in the hydroxide precursor are also in oxidation states of +2 and the ratio is determined to be 0.500:0.500. However the hydroxide precursor shows distinct XRD peaks, matching $Ni(OH)_2$ (vertical upper line,

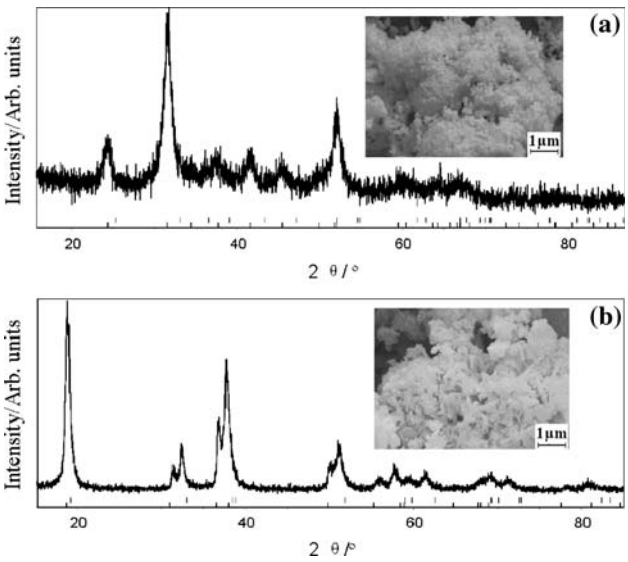

Fig. 1 X-ray diffraction patterns and SEM photograph of the precursors obtained from carbonate (**a**) and hydroxide (**b**) precipitation method respectively

JCPDS No.14-0117) and $Mn(OH)_2$ (vertical lower line, JCPDS No.18-0787) as shown in Fig. 1b. The different supersaturation points of $Ni(OH)_2$ and $Mn(OH)_2$ lead to non-synchronous aggradations of Ni^{2+} and Mn^{2+} in the hydroxide solution, which contributes to the separated hydroxide phases and inhomogeneous Ni/Mn distribution in the precursor. The degree of phase separation fluctuates in the three parallel experiments. The result is in agreement with previous studies [6, 16] and demonstrates that the synthesis of nickel manganese double hydroxides shows poor reproducibility.

The prepared precursor was also investigated by SEM. It can be seen from Fig. 1 that the size of the primary particle is on a nano-scale. The powder obtained from the carbonate precipitation process aggregates to spherical, while the sample synthesized in the hydroxide system shows sheet morphology.

3.2 End product

The average chemical compositions of the final material prepared from the precursor are $Li_{1.001}Ni_{0.499}Mn_{0.501}O_2$ and $Li_{1.021}Ni_{0.498}Mn_{0.502}O_2$, which are very close to the targeted value. The XRD patterns with Miller indices are shown in Fig. 2. All the patterns for the material are consistent with a single α-$NaFeO_2$ phase (space group *R*-3*m*). The (003)/(104) intensity ratio of >1.5 and integrated peak splits of (006)/(102) and (018)/(110) indicate that the synthesized samples have a well-development layered structure. No observable variation in the layer structure of $LiNi_{1/2}Mn_{1/2}O_2$ was detected from initial XRD analysis.

To gain insight into the microstructure, Rietveld refinement was performed. The refinement was based on detailed Bragg diffraction data using a α-$NaFeO_2$ structure model

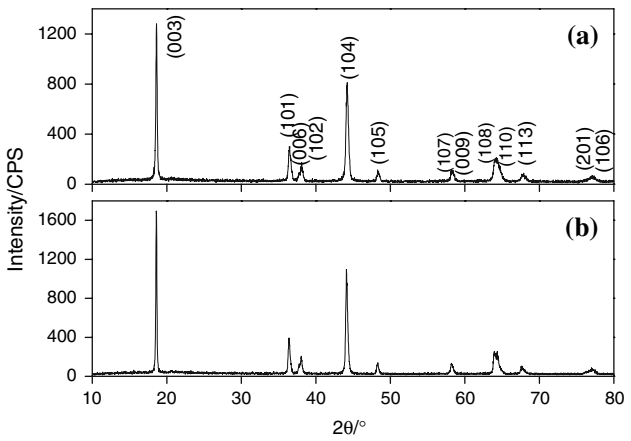

Fig. 2 X-ray diffraction patterns of the $LiNi_{1/2}Mn_{1/2}O_2$ materials synthesized from carbonate (**a**) and hydroxide (**b**) precursor respectively

with Li and some Ni on the 3a sites (0, 0, 0), transition metals and some Li on the 3b sites (0, 0, 1/2), and oxygen on the 6c sites (0, 0, z_{ox}). The refinement results and reliability factors are summarized in Table 1. As shown in Fig. 3, the calculated patterns are in good agreement with the observed patterns. The material obtained from the carbonate precursor exhibits slightly smaller lattice parameters (a = 2.886 Å, c = 14.289 Å), but a little larger $c_{hex.}/a_{hex.}$ value than for the sample prepared from the hydroxide precursor. One important finding is that for the former material the value of the Li/Ni exchange is 7.8% and smaller than that of the sample synthesized by the hydroxide precipitation method (about 8.9%). Nevertheless, the slab space distances of the samples are very similar and typically greater than 2.64 Å. Under the same fit condition $LiNi_{1/2}Mn_{1/2}O_2$ prepared in the carbonate system shows a better lamellar character with relative low mixing of cations. The complete intersolution of $NiCO_3$ and $MnCO_3$ contributes to homogeneous cation distribution in the precursor that is accessible to uniform cation distribution in transition metal (TM) layers of $LiNi_{1/2}Mn_{1/2}O_2$ and thus ideally layered with little Li/Ni disorder. On the other hand, malconformation i.e. more Ni^{2+} in some TM layers might cause greater induction in the exchange of Li^+ and Ni^{2+}.

Figure 4 shows a comparison of SEM micrographs for the as obtained $LiNi_{1/2}Mn_{1/2}O_2$ materials. The sample prepared via the carbonate co-precipitation route consists of roughly 3.5 μm spherical aggregates with primary particles with diameters around 250–300 nm. By contrast, the particles synthesized from the hydroxide precursor exhibit homogenous morphology around 450 nm in a well-shaped configuration. Small particles allow fast lithium diffusion and lead to a lower polarization, hence a higher reversible capacity in lithium cells. At the same time, the agglomerated morphology of the secondary particles is crucial to improve the tap density and volumetric capacity of electrode materials. Therefore, from a textural point of view, the carbonate co-precipitation route is favorable for the preparation of $LiNi_{1/2}Mn_{1/2}O_2$ cathode material.

Cells containing as-obtained $LiNi_{1/2}Mn_{1/2}O_2$ material were charged and discharged at a rate of 14 mA g^{-1} between fixed potential limits of 4.8 and 2.5 V. It can be seen from Fig. 5 that the samples show smooth and monotonic charge/discharge curves over the first 10 cycles. $LiNi_{1/2}Mn_{1/2}O_2$ material prepared from the carbonate precursor delivers a first discharge capacity of 190 mAh g^{-1}, which is a little lower than the previous reported value of 200 mAh g^{-1} [17]. However, irreversible capacity loss decreases to about 0.32 mAh g^{-1} per cycle after the second cycle, and reversible capacity remains at 182 mAh g^{-1} in the 10th cycle. In comparison, the material obtained from the hydroxide precursor delivers a relatively low initial reversible capacity of 177 mAh g^{-1} and a large capacity loss of 11.3% in the first 10 cycles. Clearly the

Table 1 The structure refinement results of the as obtained $LiNi_{1/2}Mn_{1/2}O_2$ materials

$LiNi_{1/2}Mn_{1/2}O_2$ Sample	Reliability factor	Lattice parameters /Å	c/a	I(003)/I(104)	Li/Ni disorder /%	Slab space of Li-O
Carbonate coprecipitation	$R_{wp} = 7.41\%$ $R_p = 5.49\%$ $R_{exp} = 5.21\%$ GOF = 1.08	a = 2.886 c = 14.289	4.95	1.578	7.8	2.648
Hydroxide coprecipitation	$R_{wp} = 7.48\%$ $R_p = 5.66\%$ $R_{exp} = 6.57\%$ GOF = 1.09	a = 2.891 c = 14.295	4.94	1.549	8.9	2.646

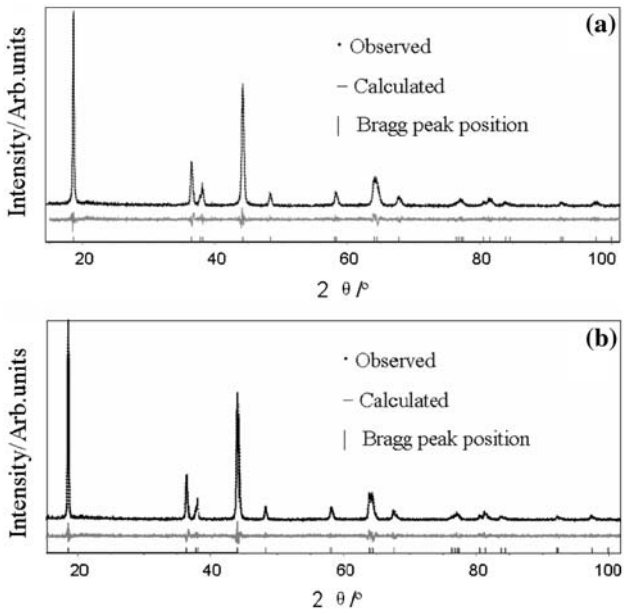

Fig. 3 Refinement results of $LiNi_{1/2}Mn_{1/2}O_2$ materials synthesized from carbonate (**a**) and hydroxide (**b**) precursor respectively

$LiNi_{1/2}Mn_{1/2}O_2$ material prepared via the carbonate co-precipitation route shows a higher reversible capacity and a better cycleability.

The amount of Ni^{2+} in the lithium layer is crucial to determining the diffusivity of Li^+ ions and the electrochemical properties of the compound [18]. Therefore, the $LiNi_{1/2}Mn_{1/2}O_2$ material obtained from carbonate co-precipitation method with low Li/Ni mixing delivers a relatively high initial capacity. For layered $LiMnO_2$, the conversion to spinel results from the migration of manganese from one layer to adjacent layers [19]. Inhomogeneous Mn ion distribution in the layer structure of $LiNi_{1/2}Mn_{1/2}O_2$ may create a larger driving force for phase transformation on cycling, which contributes to the rapid capacity loss in the material obtained from the hydroxide route. Moreover, the texture of the electrode material is important in the electrochemical behavior of Li-ion batteries. Ideal layer structure and morphology lead to the excellent electrochemical performance of $LiNi_{1/2}Mn_{1/2}O_2$ synthesized from the carbonate precursor.

4 Conclusion

Comparative study shows the influence of the precursor on $LiNi_{1/2}Mn_{1/2}O_2$ and its electrochemical performance. The precursor obtained from the carbonate co-precipitation shows a single phase with homogenous Ni and Mn distributions. The corresponding $LiNi_{1/2}Mn_{1/2}O_2$ material exhibits a large Li slab space (2.648 Å) and small Li/Ni exchange (7.8%), observed from Rietveld refinement using the Topas program. Because of its perfect layer structure and special morphology, $LiNi_{1/2}Mn_{1/2}O_2$ prepared via the carbonate co-precipitation method delivers a high reversible

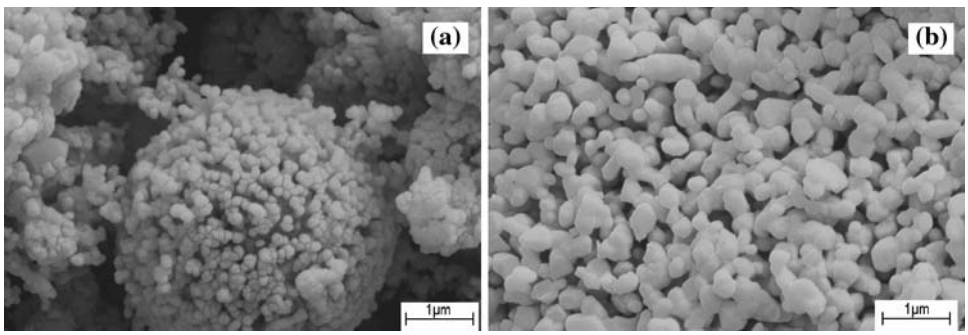

Fig. 4 SEM of $LiNi_{1/2}Mn_{1/2}O_2$ materials synthesized from carbonate (**a**) and hydroxide (**b**) precursor respectively

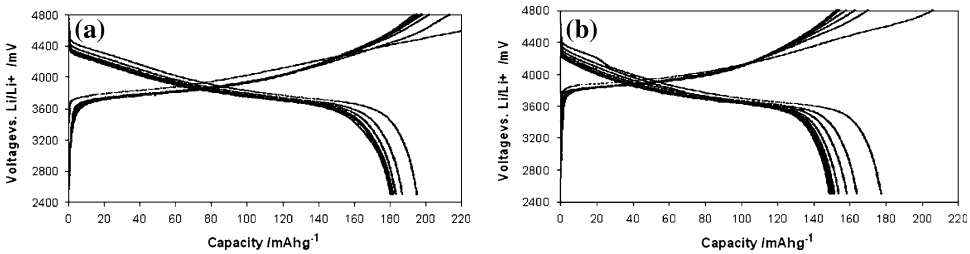

Fig. 5 The first 10 cyclic voltage profiles of $LiNi_{1/2}Mn_{1/2}O_2$ cathodes prepared from carbonate (**a**) and hydroxide (**b**) precursor at C/20 rate

capacity of 182 mAh g^{-1} in the cutoff voltage of 2.5–4.8 V and a good cycleability. In comparison, separated hydroxide phases of Ni^{2+} and Mn^{2+} in precursor contributes to inhomogeneous Ni/Mn distribution and a large Li/Ni exchange of 8.9% in $LiNi_{1/2}Mn_{1/2}O_2$. The corresponding sample synthesized with the hydroxide precipitation method exhibits a large capacity loss of 11.3% in the first 10 cycles. Therefore, the homogeneous dispersion of transition metal ions in the precursor is vital to reduce Li/ Ni disorder and improve the electrochemical performance of $LiNi_{1/2}Mn_{1/2}O_2$.

Acknowledgements The work was supported by the Ministry of Science & Technology of China (Grant No.2006BAB12B03) and the National Nature-Science Foundation of China (No.50702007).

References

1. Thackeray MM, Johnson ChS, Vaughey JT, Li N, Hackney SA (2005) J Mater Chem 15:2257
2. Kang K, Meng YS, Brèger J, Grey CP, Ceder G (2006) Science 31:977
3. Myung ST, Komaba Sh, Kumagai N (2004) Solid State Ionics 170:139
4. Rossen E, Jones CDW, Dahn JR (1992) Solid State Ionics 57:311
5. Li DCh, Sasaki Y, Kageyama M, Kobayakawa K, Sato Y (2005) J Power Sources 148:85
6. Ohzuku T, Makimura Y (2001) Chem Lett 744
7. Ammundsen B, Paulsen J (2001) Adv Mater 13(12–13):943
8. Spahr ME, Novák P, Schnyder B, Haas O, Nesper RJ (1998) J Electro Chem 145:1113
9. Makimura Y, Ohzuku T (2003) J Power Sources 119–121:156
10. Lu ZhH, Beaulieu LY, Donaberger RA, Thomas CL, Dahn JR (2002) J Electrochem Soc 149:A778
11. Whittingham MS (2004) Chem Rev 104:4271
12. Cho TH, Park SM, Yoshio M, Hirai T, Hideshima Y (2005) J Power Sources 142:306
13. Shin HS, Park SH, Bae YC, Sun YK (2005) Solid State Ionics 176:2577
14. Chitrakar R, Kasaishi S, Umeno A, Sakane K, Takagi N, Kim YS, Ooi K (2002) J Solid State Chem 169:35
15. Barkhouse DAR, Dahn JR (2005) J Electrochem Soc 152:A746
16. Tran N, Croguennec L, Jordy C, Biensan Ph, Delmas C (2005) Solid State Ionics 176:1539
17. Park YJ, Hong YS, Wu XL, Ryu KS, Chang SH (2004) J Power Sources 129:288
18. Breger J, Duprè N, Chupas PJ, Lee PL, Proffen Th, Parise JB, Grey CP (2005) J Am Chem Soc 127:7529
19. Van der Ven A, Ceder G (2004) Electrochem Commun 6:1045